Evaluation of the SWAT model performance for simulating river discharge in the Himalayan and tropical basins of Asia

Sangam Shrestha, Manish Shrestha and Pallav Kumar Shrestha

ABSTRACT

This study evaluated the Soil and Water Assessment Tool (SWAT) model performance for 11 basins located in two contrasting climatic regions of Asia: the Himalayan and the Southeast Asian tropics. A large variation existed among the case study basins in relation to basin size (330–78,529 km^2), topography (377–4,310 metres above sea level) and annual rainfall (1,273–2,500 mm). Performance of the model was evaluated using R^2 and wR^2 for a low discharge event; Nash–Sutcliffe efficiency (NSE), R^2 and $RMSE$-observation standard deviation ratio (RSR) for high discharge events; and NSE, R^2, $PBIAS$, RSR, NSE_{rel} and wR^2 for the overall hydrographs. SWAT was found to be suitable for both climatic regions but yielded better performance in the Himalayan basins (NSE 0.72–0.81 at calibration) compared to the tropical basins (NSE 0.36–0.72 at calibration). Although most of the models underperformed in either low or high discharge events, a few of those remaining showed a balance between the extremes, proving that it is possible to achieve a balanced hydrograph with the SWAT model. The consistency of model performance across numerous Himalayan and tropical basins in the area confirmed the versatility and reliability of SWAT as a hydrological model and suitable tool for water resources planning and management.

Key words | Himalayan basins, model evaluation, river discharge, SWAT, tropical basins

Sangam Shrestha (corresponding author)
Manish Shrestha
Pallav Kumar Shrestha
Water Engineering and Management,
Asian Institute of Technology,
Klong Luang,
Pathumthani 12120,
Thailand
E-mail: *sangam@ait.asia*

INTRODUCTION

The Soil and Water Assessment Tool (SWAT) is a physically based, spatially distributed, continuous time hydrological model that has been successfully applied worldwide for the assessment and management of water resources and nonpoint source pollution problems, over a wide range of scales, topographies and climate conditions (Arnold *et al.* 2012; Grusson *et al.* 2015; Francesconi *et al.* 2016). With an open access policy and detailed documentation, SWAT is presently a widespread and recognised hydrological model among water researchers and its application has been both successful and extensive (Krysanova & White 2015). In view of the contemporary issues related to climate change impact on snow-dominant hydrology and extreme hydrological events, two contrasting regions – the mid-latitude Himalayan and Southeast Asian tropics – were selected for the evaluation of SWAT to simulate streamflow.

One of the major advantages of SWAT is its ability to model ungauged or poorly gauged watersheds (Arnold *et al.* 1998). This makes it attractive for use in developing countries with inadequate infrastructures to measure the required inputs for hydrologic and nonpoint source pollution modelling. Several individual studies show that the SWAT model is successful in simulating the hydrological behaviour of both Himalayan and tropical basins. Many studies show the successful application of the SWAT model in Alpine regions as well (Abbaspour *et al.* 2007; Majone *et al.* 2010; Dobler *et al.* 2012; Grusson *et al.* 2015). Similar good results have been reported for Himalayan

doi: 10.2166/nh.2017.189

basins (Singh *et al.* 2011; Neupane *et al.* 2014, 2015; Shrestha *et al.* 2017). Successful applications in tropical basins have also been registered through various SWAT-based hydrological research works (Ndomba *et al.* 2008; Beskow *et al.* 2011; Plesca *et al.* 2012; Cornelissen *et al.* 2013; Aung *et al.* 2015; Pereira *et al.* 2016; Rocha 2016; Rodrigues 2016; Yira *et al.* 2016). However, conclusive research on model suitability in contrasting climatic regions via the multi-basin evaluation approach is seldom found in the literature. Moreover, evaluation of model-simulated discharge is usually based on a handful of statistics, missing any dissected evaluation of specific hydrograph portions such as the effect of snow-dominant hydrology on the Himalayan basins and hydrological extremes in tropical basins.

This study evaluates the suitability of the SWAT model for river discharge simulation in the Himalayan and tropical regions of Asia via the multi-basin evaluation approach. Five Himalayan basins and six tropical basins in the Southeast Asian tropics have been selected for SWAT model evaluation. The study area varies significantly in basin size (330–78,529 km^2), topography (377–4,310 metres above sea level) and annual rainfall (1,273–2,500 mm).

METHODS

Description of study area

Five Himalayan basins and six tropical basins were selected for this study (Figure 1). The Himalayan basins include: Indrawati, Melamchi, Tamakoshi, Tamor and Kathmandu and the tropical basins include: Bago, Belu, Sekong, Sesan, Srepok and the 3S River Basin. As shown in Table 1, the study area lies within latitude 12 °N–28 °N

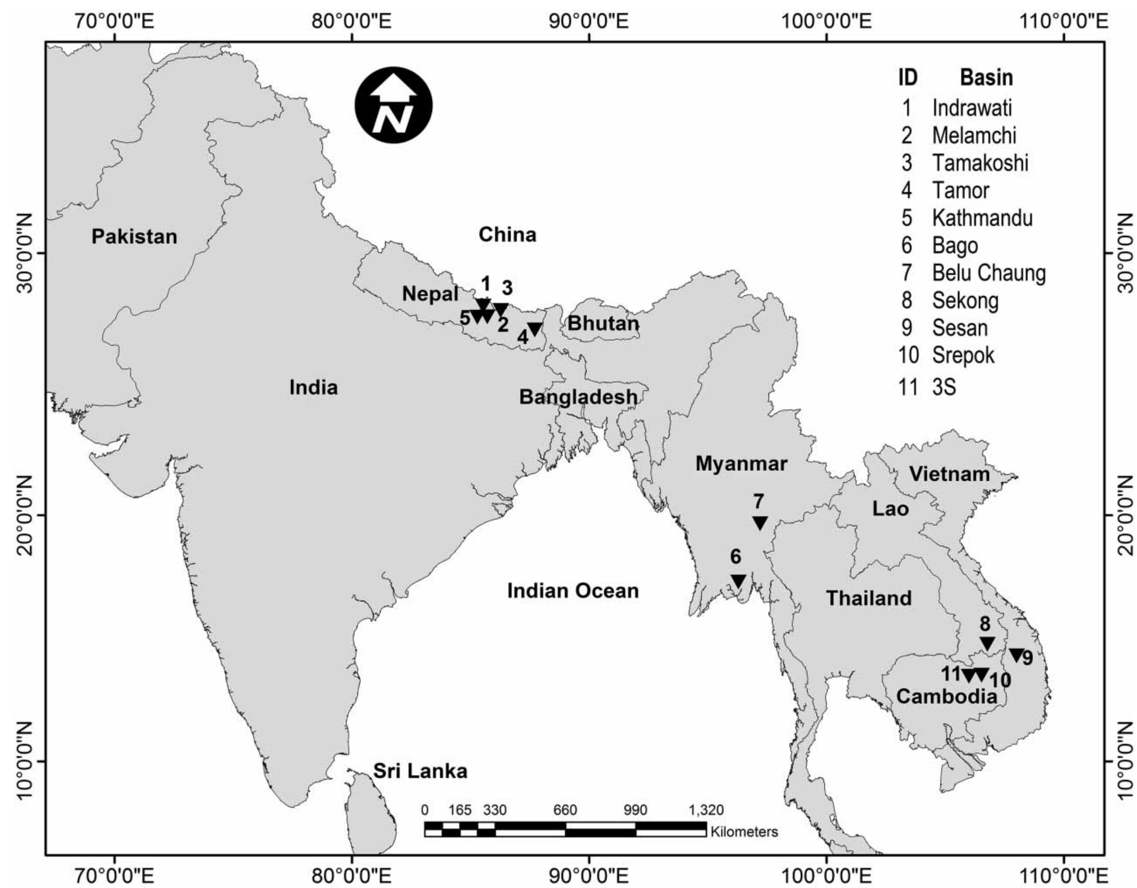

Figure 1 | Location map of study basins in the Himalayan and tropical regions.

Table 1 | Physiographic and climatic characteristics of selected study basins

No.	Basin, country	Location Lat.	Long.	Area (km^2)	Altitude (masl)	Rainfall (mm/yr)
Himalayan						
1	Indrawati, Nepal	27.64	85.71	1,230	3,200	2,000
2	Melamchi, Nepal	28.04	85.53	330	2,134	2,000
3	Tamakoshi, Nepal	27.88	86.27	2,926	4,082	1,900
4	Tamor, Nepal	27.15	87.71	4,377	4,310	1,925
5	Kathmandu, Nepal	27.63	85.29	664	1,350	2,000
Tropical						
6	Bago, Myanmar	17.33	96.29	4,883	377	2,500
7	Belu Chaung, Myanmar	19.66	97.20	8,329	760	1,273
8	Sekong, Laos	14.81	106.78	28,766	1,101	1,840
9	Sesan, Vietnam	14.34	108.01	18,684	1,210	1,840
10	Srepok, Cambodia	13.55	106.53	31,079	1,199	1,890
11	3S (Laos, Cambodia and Vietnam)	13.50	106.00	78,529	1,060	2,450

and longitude 84°E–110°E and covers the basin from Nepal, Myanmar, Laos, Vietnam and Cambodia. The area of the basin ranges from 330 km^2 (Melamchi RB, Nepal) to 78,529 km^2 (3S RB, Laos, Cambodia and Vietnam). The physiographic and climatic characteristics vary significantly among the basins. The altitude of the basins ranges from 760 metres above sea level (masl) (Belu Chaung, Myanmar) to 4,310 masl (Tamor, Nepal) and the average annual rainfall fluctuates from 1,900 mm (Tamakoshi, Nepal) to 2,500 mm (Bago, Myanmar). On average, 80% of the total rainfall occurs during the monsoon season (May–September).

Data used

The input requirement for SWAT includes meteorological data, land use, land cover, soil properties and topography (Shrestha *et al.* 2016). The meteorological data required on a daily basis include rainfall, maximum and minimum temperature, relative humidity (RH), solar radiation and wind speed, all of which were collected from the meteorological departments of the respective countries (Table 2). As most of the regions covered were located in developing countries, the issue of data continuity persisted. However, SWAT includes a provision for weather generation using its inbuilt stochastic weather generator model (WXGEN) to deal with missing days. The climate statistics for WXGEN include average and standard deviations of precipitation, maximum and minimum temperature for each month, probability of wet days, average solar radiation, wind speed, dew point temperature and skew coefficient of precipitation. Based on these statistics and WXGEN, SWAT generates rainfall and temperature for missing days at all stations. The solar radiation and RH are generated based on the presence and absence of rainfall for a particular day, before finally generating wind speed independently (see Neitsch *et al.* 2011 for more details). The digital elevation model (DEM) used for the study at 30 m resolution was collected from the Advanced Spaceborne Thermal Emission and Reflection Radiometer (ASTER), except for Bago basin which was collected from the Shuttle Radar Topography Mission (SRTM) at 90 m resolution. The soil map for the Nepalese basins was obtained from the Soil and Terrain Database (SOTER) whereas the Digital Soil Map of the World (DSMW) was used for the basins in Myanmar. The land use information for the basins in these two countries was abstracted from the global database of the European Space Agency (ESA) except for Tamor which utilised the local land use map from the relevant government department. In the case of the 3S River Basin (including Sekong, Sesan and Srepok),

Table 2 | Summary of data and its corresponding resolution and sources

Spatial data

	DEM[a]		Land use map		Soil map	
Basin, country	**Resolution**	**Source**	**Resolution**	**Source**	**Scale/Resolution**	**Source**
Indrawati, Nepal	30 m	ASTER[b]	300 m	ESA	1:1,000,000	SOTER
Melamchi, Nepal	30 m	ASTER	300 m	ESA	1:1,000,000	SOTER
Tamakoshi, Nepal	30 m	ASTER	300 m	ESA	1:1,000,000	SOTER
Tamor, Nepal	30 m	ASTER	1:50,000	Srv Dept.	1:1,000,000	SOTER
Kathmandu, Nepal	90 m	ICIMOD	30 m	ESA	1:1,000,000	SOTER
Bago, Myanmar	90 m	SRTM[c]	300 m	ESA	1:1,000,000	DSMW
Belu Chaung, Myanmar	30 m	ASTER	300 m	ESA	1:1,000,000	DSMW
Sekong, Laos	250 m	MRC	250 m	MRC	250 m	MRC
Sesan, Vietnam	250 m	MRC	250 m	MRC	250 m	MRC
Srepok, Cambodia	250 m	MRC	250 m	MRC	250 m	MRC
3S (Laos, Cambodia and Vietnam)	250 m	MRC	250 m	MRC	250 m	MRC

Meteorological data

	No. of stations				
Basin, country	**Rainfall**	**Temp.**	**RH, wind speed, solar radiation**	**Period**	**Source**
Indrawati, Nepal	6	1	–	1992–2009	DHM[d], Nepal
Melamchi, Nepal	6	1	–	1992–2009	
Tamakoshi, Nepal	2	1	–	2000–2008	
Tamor, Nepal	9	4	2	2000–2006	
Kathmandu, Nepal	11	3	–	1999–2009	
Bago, Myanmar	3	3	–	1994–2008	DMH[e], Myanmar
Belu Chaung, Myanmar	9	6	–	1976–2005	
Sekong, Laos	16	6	6	1994–2008	MRC
Sesan, Vietnam	16	6	6	1994–2008	
Srepok, Cambodia	16	6	6	1994–2008	
3S (Laos, Cambodia and Vietnam)	16	6	6	1994–2008	

[a]DEM = digital elevation model.
[b]SRTM = Shuttle Radar Topography Mission.
[c]ASTER = Advanced Spaceborne Thermal Emission and Reflection Radiometer.
[d]DHM = Department of Hydrology and Meteorology, Nepal; Srv Dept. = Survey Department, Nepal.
[e]DMH = Department of Meteorology and Hydrology, Myanmar; MRC = Mekong River Commission.

meteorological, land use and soil maps were provided by the Mekong River Commission (MRC).

SWAT model

The Arc-SWAT is a semi-distributed hydrological model incorporated into an ArcGIS interface. The SWAT model consists of hydrological, sedimentation/erosion, weather, plant growth, nutrients, land management, channel routing and pond/reservoir routing components. However, in this study, the hydrological, weather and channel routing components were used. The water cycle in the SWAT model is based on the water balance equation shown below:

$$SW_t = SW_o + \sum (R_{day} - Q_{surf} - E_a - W_{seep} - Q_{gw}) \tag{1}$$

where SW_t is the final soil water content, SW_0 is the initial soil water content, t is time in days, R_{day} is the amount of precipitation, Q_{surf} is the amount of surface runoff, E_a is the amount of evapotranspiration, W_{seep} is the amount of water entering the vadose zone from the soil profile and Q_{gw} is the amount of return flow. All are expressed in millimetres.

The snow component of the SWAT is estimated through a degree-day approach. The snowfall is stored at the surface in the form of a snowpack. The mass balance for a snowpack in the model is provided in Equation (2):

$$SNO = SNO + R_{day} - E_{sub} - SNO_{mlt} \tag{2}$$

where SNO is the total amount of water in the snowpack on a given day (mm H_2O), R_{day} is the amount of precipitation (mm H_2O), E_{sub} is the amount of sublimation (mm H_2O) and SNO_{mlt} is the amount of snowmelt (mm H_2O). The melting of snow is the function of air temperature, degree-day factor and the threshold value of the ice melt. For more information on water balance and the snow component, please refer to Neitsch et al. (2011).

The general framework of the SWAT modelling approach adopted in this study is shown in Figure 2. The basic data required to set up a SWAT model consist of DEM, land use, soil map and climate data such as rainfall, temperature (max and min), RH, solar radiation and wind speed. However, climate data in many regions are not always available or may be of low quality or with values missing. In this case, the SWAT model consists of a built-in stochastic weather generator model (WXGEN) to generate and fill in missing, measured data. Therefore, the SWAT model can also be used to simulate the hydrology in an ungauged or data-scarce area.

The watershed of any model is first divided into a number of sub-basins and then further divided into hydrological response units (HRUs). SWAT forms the HRUs based on similar land use, soil type and slopes (Shrestha et al. 2016) which are areas in the watershed which respond similarly to given inputs such as rainfall and temperature (Neitsch et al. 2011). Elevation data, land use and soil data are used to drive discharges and direct sub-basin routing (Easton et al. 2010). All the hydrological processes are simulated in HRUs. SWAT consists of numerous parameters (such as snowfall, temperature, soil, groundwater, etc., related parameters) that govern the response of the model. These parameters were calibrated either manually or by using an automated calibration tool (SWAT-CUP) so that the simulated

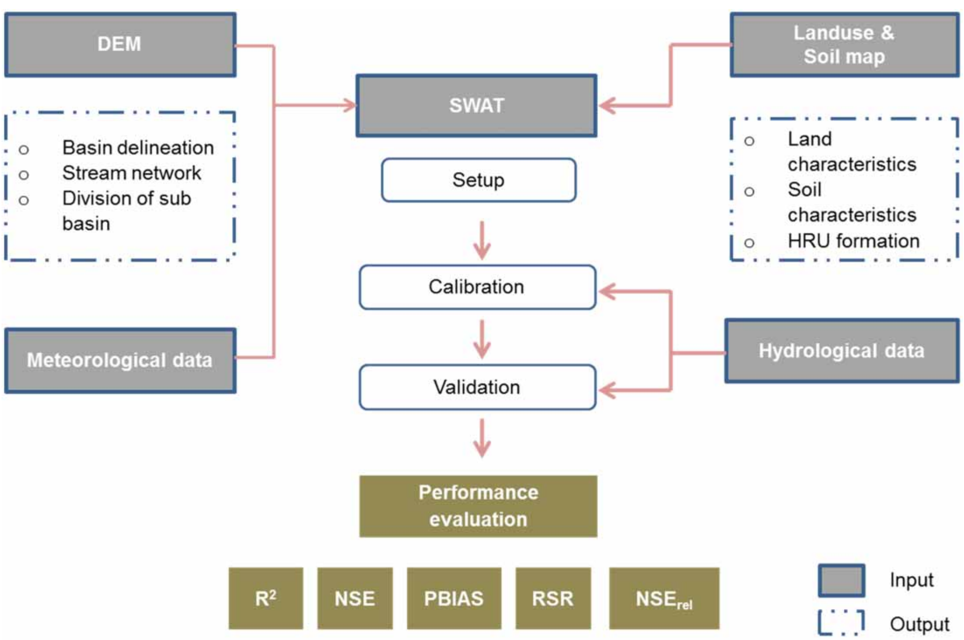

Figure 2 | General framework of the SWAT modelling approach adopted in this study.

discharge is close to the observed discharge. The calibrated model was then run using a new set of data for its validation.

Calibration and validation

SWAT parameters are process-based and must be within a realistic uncertainty range (Arnold *et al.* 2012). Sensitivity analysis was performed to determine the most appropriate parameters for a given watershed. In some basins, it was performed by changing one parameter value at a time (local approach), whereas in others the SWAT-CUP tool (global approach) was used. The sensitive parameters were then used to calibrate the model against the observed discharge data. A manual calibration was performed in some basins and auto-calibration using an automated calibrating tool (SWAT-CUP) in others. Model validation was conducted to ensure its accurate simulation capability using new sets of input data. The calibration and validation period for each basin is shown in Table 3.

The two contrasting applications for model parameterisation and calibration each have pros and cons. Manual calibration offers a one parameter at a time approach wherein the sensitivity of the model is checked by the fluctuating value of a single parameter. The modified value reverts back unless a significant improvement in evaluation statistics and hydrography is observed (refer to next section on model performance evaluation). Although computationally less demanding, this approach has many drawbacks; it is more time-consuming and inter-parameter sensitivity is hard to track (sensitivity of one parameter through a range in value of another parameter). In the case of automatic calibration using the SWAT-CUP optimisation tool, parameter sets with randomly selected values are generated to obtain multiple runs (usually 500–1,500 runs), eliminating the drawbacks of manual calibration. The drawbacks of this approach include the cost for its licensed use, time required for setting up the analysis, and higher computational requirements. However, if a set of sensitive parameters were to be available along with the value range for similar geographical and climatological regions, manual calibration is the relatively easier option.

All the models were calibrated against the observed discharge at the basin outlet with the exception of the 3S River Basin. The Sekong River, Sesan River and Srepok River are collectively called the 3S River Basin. In the 3S River Basin, the model was calibrated in each of the three rivers and at their confluence. The calibration is usually taken over a longer period so that the model can properly capture the physical parameters and the long-term trends. For this study, the calibration period is taken as roughly 60% of the total data available.

Table 3 | Model calibration and validation period for selected study basins

Basin, country	Available data	Period	
		Calibration	Validation
Indrawati, Nepal	2006–2009	2006–2008	2009
Melamchi, Nepal	1990–2008	1992–2003	2004–2008
Tamakoshi, Nepal	2000–2008	2004–2008	2000–2001
Tamor, Nepal	2000–2006	2000–2003	2004–2006
Kathmandu, Nepal	2003–2006	2003–2004	2005–2006
Bago, Myanmar	1994–2008	1994–2003	2004–2008
Belu Chaung, Myanmar	1976–2005	1976–1990	1991–2005
Sekong, Laos	2001–2005	–	2001–2005
Sesan, Vietnam	1994–2005	2000–2005	1994–1999
Srepok, Cambodia	2000–2008	2000–2004	2005–2008
3S (Laos, Cambodia and Vietnam)	2000–2008	2000–2004	2005–2008

Model performance evaluation

In this study, both graphical and statistical methods are used to determine the model performance in an attempt to evaluate the hydrological behaviour (i.e., discharge data) more completely. The error monitoring parameters were selected in such a way that the set of criteria checks both water balance as well as extreme events of the discharge data. To evaluate the performance of models for water balance, statistical parameters such as the coefficient of determination (R^2), NSE, percentage bias ($PBIAS$), RSR and relative Nash–Sutcliffe efficiency (NSE_{rel}), along with the visual hydrographs were selected as recommended by Moriasi *et al.* (2007) and Krause *et al.* (2005). Furthermore, the top and bottom 5% slices of the discharge distribution were then evaluated to check the model performance in simulating extreme events. For the 5% peak discharge, R^2, NSE and RSR

were utilised, whereas for the bottom 5%, low discharge R^2 and weighted R^2 (wR^2) were used. In addition to all the statistical measures, flow duration curves (FDCs) and quantile box plots were employed as graphical measures to illustrate the SWAT model performance in replicating the extreme values of discharge. A brief description of each statistical parameter is set out below.

R^2 (Coefficient of determination)

R^2 estimates the combined dispersion against the single dispersion of the observed and predicted series and provides the relationship strength between observed and simulated values. Its value ranges from 0 to 1; a value close to 0 means very low correlation whereas a value close to 1 represents high correlation between observed and simulated discharge.

$$\mathrm{R}^2 = \frac{\left[\sum_{i=1}^{n}(Q_i - \overline{Q_i})\cdot(Q_i' - \overline{Q_i'})\right]^2}{\sum_{i=1}^{n}(Q_i - \overline{Q_i})^2 \cdot \sum_{i=1}^{n}(Q_i' - \overline{Q_i'})^2} \quad (3)$$

NSE (Nash–Sutcliffe efficiency)

NSE determines the relative magnitude of the residual variance compared to that of the measured data (Moriasi *et al.* 2007) and is one of the most widely used statistical indicators for hydrological model performance (Shrestha *et al.* 2013). Its value ranges from $-\infty$ to 1, where 1 indicates a perfect model and a value of less than 0 indicates that the mean value of the observed time series would have been a better predictor than the model.

$$\mathrm{NSE} = 1 - \frac{\sum_{\mathrm{i}=1}^{\mathrm{n}}(Q_i - Q_i')^2}{\sum_{\mathrm{i}=1}^{\mathrm{n}}(Q_i - \overline{\mathrm{Q}}_{\mathrm{i}})^2} \quad (4)$$

PBIAS (percentage bias)

PBIAS indicates the average tendency of the simulated results to be greater or larger than their observed data. It measures the difference between the simulated and observed quantity and its optimum value is 0. The positive value of the model represents underestimation whereas negative value represents overestimation.

$$\mathrm{PBIAS} = \frac{\sum_{\mathrm{i}=1}^{\mathrm{n}}(Q_i - Q_i')}{\sum_{\mathrm{i}=1}^{\mathrm{n}} Q_i} * 100 \quad (5)$$

RSR (RMSE-observation standard deviation ratio)

The lower value of *RMSE* (root mean square error) is commonly acceptable and one of the widely used error parameters. However, the satisfactory threshold of *RMSE* is case specific. Therefore, *RSR* is chosen as a complementary indicator to *RMSE*. The optimum value of *RSR* is 0 and higher value indicates lower model performance.

$$\mathrm{RSR} = \frac{\mathrm{RMSE}}{\mathrm{STDEV_{obs}}} = \frac{\sqrt{\sum_{i=1}^{n}(Q_i - Q'_i)^2/n}}{\sqrt{\sum_{\mathrm{i}=1}^{\mathrm{n}}(Q_i - \bar{Q}_i)^2/n}} \quad (6)$$

$\mathrm{NSE_{rel}}$ (relative Nash–Sutcliffe efficiency)

According to Krause *et al.* (2005), *NSE* quantifies the difference between the observation and prediction of absolute values whereby an over- or underprediction generally has a greater influence on higher rather than lower values. This reaction to peak values (discharge) could be suppressed by the derivation of the relative form of *NSE* as shown in the following expression. Krause *et al.* (2005) found NSE_{rel} to be sensitive to low discharge only and not reactive to peak discharge at all, making it an ideal statistic for evaluating the base discharge simulation performance of a hydrological model.

$$\mathrm{NSE_{rel}} = 1 - \frac{\sum_{\mathrm{i}=1}^{\mathrm{n}}(Q_i - Q_i'/Q_i)^2}{\sum_{\mathrm{i}=1}^{\mathrm{n}}(Q_i - \bar{\mathrm{Q}}_{\mathrm{i}}/\bar{\mathrm{Q}}_{\mathrm{i}})^2} \quad (7)$$

wR^2 (weighted coefficient of determination)

R^2 quantifies only the ability of the model to explain the dispersion present in the observed data. Therefore, if the model under- or overestimates, at all times maintaining the pattern of the hydrograph, it will still result in good R^2 values. Krause *et al.* (2005) advise taking into account the gradient

b of the regression on which R^2 is based. For good modelling results, b should be close to 1, and if not, this will be captured by the following expression of weighted R^2.

$$\mathrm{wR}^2 = \begin{cases} |\mathrm{b}|{*}\mathrm{R}^2 & \text{for b} \leq 1 \\ |\mathrm{b}|^{-1}{*}\mathrm{R}^2 & \text{for b} > 1 \end{cases} \tag{8}$$

where Q_i = measured daily discharge, Q_i' = simulated daily discharge, $\bar{Q}_i$ = average daily discharge for observed period, $\bar{Q}_i'$ = average daily discharge for simulated period, n = number of daily discharge values, $STDEV_{obs}$ = standard deviation of measured discharge.

The threshold value of goodness-of-fit for all models was based on Moriasi *et al.* (2007), as shown in Table 4.

RESULTS AND DISCUSSION

Evaluation of SWAT in the Himalayan basins

General hydrology

The SWAT models for the Himalayan basins were calibrated against the discharge data at the basin outlet of each watershed, as depicted in Table 5. The Indrawati model shows a slight underestimation whereas the Tamor model has slightly overestimated the discharge during the calibration period. However, all the basins show good agreement between the simulated and observed discharge. During the calibration period, the *NSE* and R^2 models range from 0.72 to 0.81 and 0.76 to 0.83, respectively. These figures correspond to a 'very good' rating and thus show that the SWAT model is capable of capturing both the daily variation and pattern of discharge. Similarly, *PBIAS* and *RSR* also fall within the rating of 'good' with values ranging from −14.8 to 11.62% and 0.19 to 0.53, respectively.

In the validation period, for Melamchi and Kathmandu, the statistics show underperformance compared to the calibration period. Looking into the hydrographs for these two basins (Figure 3), it is noted that the observed hydrograph in the validation portion has more varied features for some of the years than those covered by calibration. For instance, in Melamchi, the inability of the model to match the low discharge for 2006 and 2008 has influenced the model performance statistics, while for Kathmandu, the annual volume discharge in the validation period is visibly much less than for the calibration years. However, the models for Indrawati, Tamor and Tamakoshi show a good or better performance compared to the calibration period. This shows that as long as good decisions are made in the selection of calibration and validation years and duration, the SWAT model fits well hydrographically, with a high-performance rating.

Of the five basins, apart from Kathmandu, the remaining are snow-fed watersheds, adding one more hydrological process, and thus complexity, to the model. Of the indicators,

Table 4 | Model performance rating based on Moriasi *et al.* (2007)

Performance rating	*NSE*	*PBIAS*	*RSR*
Very good	0.75	<± 10	0 to 0.5
Good	0.65 to 0.75	±10 to ±15	0.5 to 0.6
Acceptable	0.5 to 0.65	15 to ±25	0.6 to 0.7
Unsatisfactory	<0.5	>± 25	>0.7

Table 5 | Goodness-of-fit statistics for general daily discharge simulated by the SWAT model in the Himalayan river basins

	Calibration					Validation				
Basin	*NSE*	R^2	*PBIAS (%)*	*RSR*	NSE_{rel}	*NSE*	R^2	*PBIAS (%)*	*RSR*	NSE_{rel}
Indrawati, Nepal	0.81	0.83	11.62	0.19	0.69	0.87	0.90	3.37	0.19	0.79
Melamchi, Nepal	0.76	0.76	2.17	0.35	0.59	0.55	0.58	2.15	0.36	0.67
Tamakoshi, Nepal	0.76	0.76	−1.69	0.53	0.75	0.84	0.85	5.24	0.28	0.90
Tamor, Nepal	0.72	0.79	−14.8	0.53	0.91	0.78	0.79	−6.5	0.47	0.90
Kathmandu, Nepal	0.81	0.86	6.21	0.43	0.81	0.52	0.69	−8.68	0.69	0.70

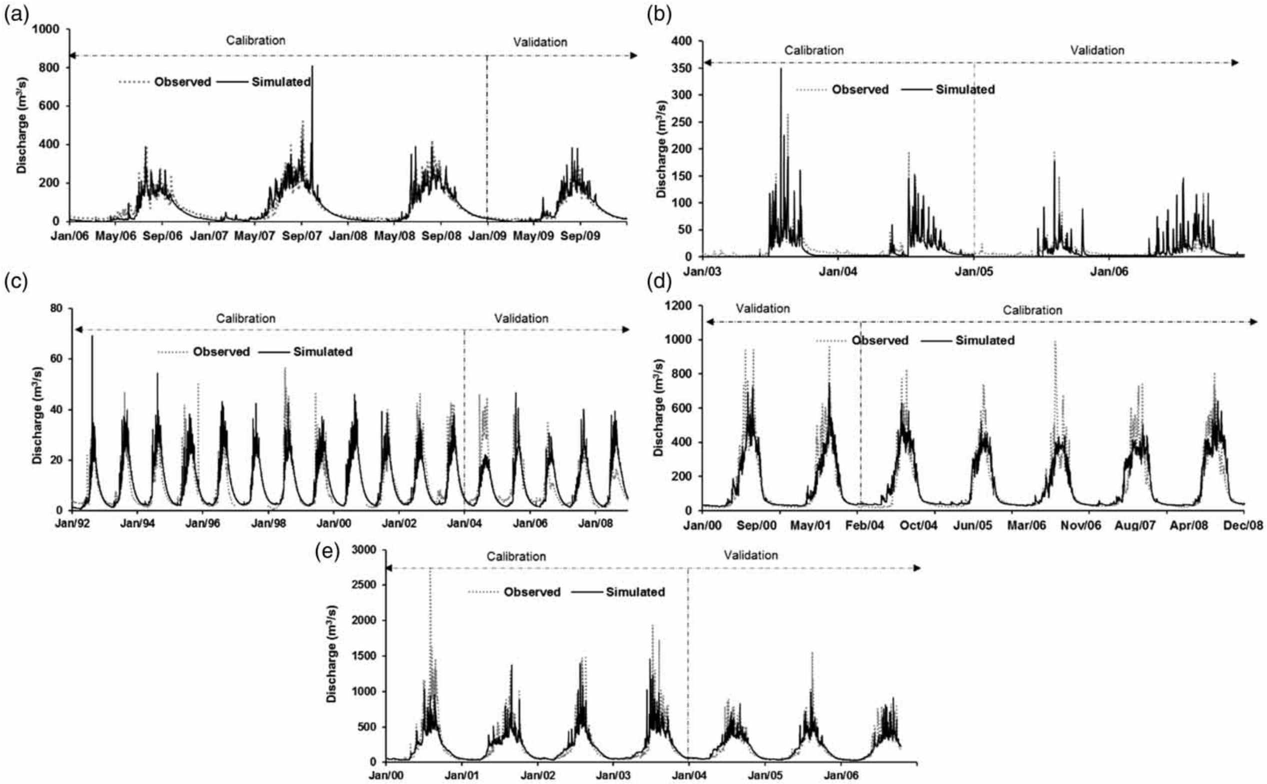

Figure 3 | Observed and simulated daily river discharge during calibration and validation of the SWAT model in the Himalayan basins: (a) Indrawati, (b) Kathmandu Valley, (c) Melamchi, (d) Tamor and (e) Tamakoshi.

PBIAS, R^2 and NSE_{rel} help in controlling simulations with snow-fed hydrology. *PBIAS* checks the annual volume/water balance effect of snow, R^2 checks the induced seasonality pattern, while NSE_{rel} helps to check the snowmelt contribution in low discharge periods. *PBIAS* has improved in all these four basins in the validation period, falling into the 'very good' range, indicating good water balance agreement with the SWAT simulations. Whereas for the major snow-fed basins – Tamor and Tama Koshi – R^2 and NSE_{rel} show high-performance values throughout the modelling years as well. These results support the SWAT model's ability to reproduce the hydrological variation brought about by the snow component.

The overall impression is that all five SWAT models for the Himalayan basins performed very well in calibration. All statistics were satisfied and the hydrograph matched well. The performance of two models degraded during validation which may be attributed to the selection of modelling periods.

Hydrological extremes

For the evaluation of SWAT to simulate the extreme discharge values, the top and the bottom 5% of discharge were selected. The bottom 5% (*Q95*, i.e., discharge exceeds this value 95% of the time) is evaluated using R^2 and wR^2. R^2 helps to evaluate the pattern of low discharge while wR^2 assists in checking the R^2 bias. A good performance of low discharge yields was in the high range for both indices in the Melamchi, Tamor and Tamakoshi Basins. The degraded wR^2 values for Indrawati and Kathmandu indicates an underestimation of low discharge, although an acceptable range for R^2 may have been achieved.

On the other hand, the top 5% (*Q5*, i.e., discharge exceeds this value only 5% of the time) is evaluated using *NSE*, R^2 and *RSR*. *NSE* and *RSR* are added to help check the peak variations among the flood events. As seen from the hydrograph (Figure 3), in addition to the high-performance statistics, the SWAT model for Kathmandu is seen as highly effective in simulating peak discharge. Considering a liberal range for the extreme value statistics, a good match in the Indrawati and Melamchi basins can be implied. Although the pattern of the peaks has been captured for the remaining two basins, the models have lagged in simulating the sharp magnitude of such events.

Two of the five SWAT models at the Himalayan basins – Tamor and Tamakoshi – seem to have focused on matching the base flow (consisting of *Q95*), while two others at Indrawati and Kathmandu have peak matching hydrograph outputs (Table 6). This is also evident from the FDCs and quantile box plots, as shown in Figure 4. The starting end of the FDC and bottom whiskers of the box plots for Tamor and Tamakoshi show very close agreement with that of the observed, while the rising end of the FDC and upper whiskers show closer results for Indrawati and Kathmandu. In the SWAT model for Melamchi, all of these are seen to be toning (whiskers of the box plots or the start and end portions of its FDC) resulting in a balance between the two hydrological extremes. Thus, it was found that a highly accurate hydrograph is possible using SWAT for flood events, low discharge or a balance between the two. However, although successful in extremes, the middle portion of the FDC for Melamchi (representing general discharge between 5 and 95%) shows a distinct mismatch, as previously discussed.

Table 6 | Goodness-of-fit statistics of daily hydrological extremes simulated by the SWAT model in the Himalayan river basins

	Low discharge (*Q95*) statistics		High discharge (*Q5*) statistics		
Basin	R^2	wR^2	*NSE*	R^2	*RSR*
Indrawati (Nepal)	0.327	0.056	0.459	0.806	0.735
Melamchi (Nepal)	0.958	0.925	0.380	0.948	0.788
Tamakoshi (Nepal)	0.940	0.685	−0.852	0.981	1.361
Tamor (Nepal)	0.983	0.767	−0.459	0.965	1.208
Kathmandu Valley (Nepal)	0.540	0.005	0.889	0.939	0.332

Evaluation of SWAT in tropical basins

General hydrology

The SWAT model was also calibrated against the discharge data at the outlet of each watershed in the tropical basins (refer to Table 7 and Figure 5). In general, the model shows good agreement between the simulated and observed discharge for all basins. However, the model shows the highest underestimation for the Sesan

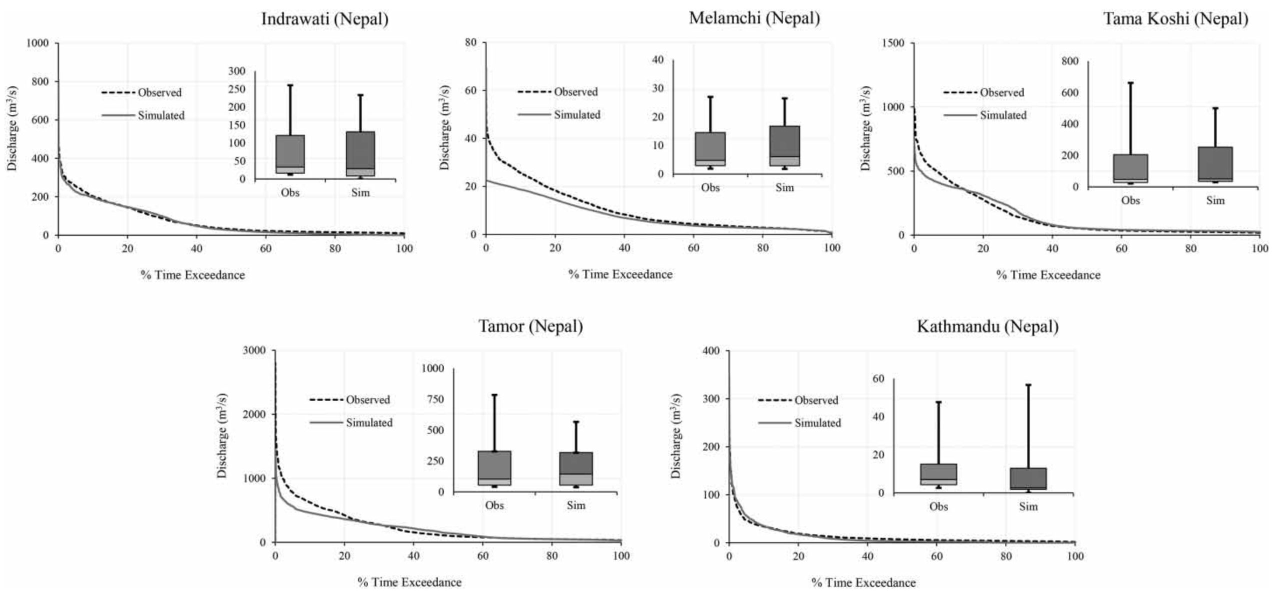

Figure 4 | Observed and simulated daily FDCs and quantile box plots for river discharge in the Himalayan basins.

Table 7 | Goodness-of-fit statistics of general daily discharge simulated by the SWAT model in the tropical river basins

	Calibration					Validation				
Basin	***NSE***	***R²***	***PBIAS* (%)**	***RSR***	***NSE_rel***	***NSE***	***R²***	***PBIAS* (%)**	***RSR***	***NSE_rel***
Belu, Myanmar	0.53	0.56	0.05	0.68	−1.41	0.70	0.75	−0.09	0.54	−0.63
Bago, Myanmar	0.69	0.70	5.40	0.21	0.87	0.81	0.82	4.54	0.15	0.93
Sekong, Laos	–	–	–	–	–	0.80	0.80	8.01	0.19	0.79
Sesan, Vietnam	0.36	0.60	−9.56	0.41	0.40	0.60	0.58	24.41	0.18	0.72
Srepok, Cambodia	0.54	0.54	−6.9	0.33	−0.17	0.57	0.58	−3.82	0.25	−1.49
3S (Laos, Cambodia and Vietnam)	0.72	0.72	8.21	0.21	−5.22	0.68	0.68	−2.86	0.36	−17.71

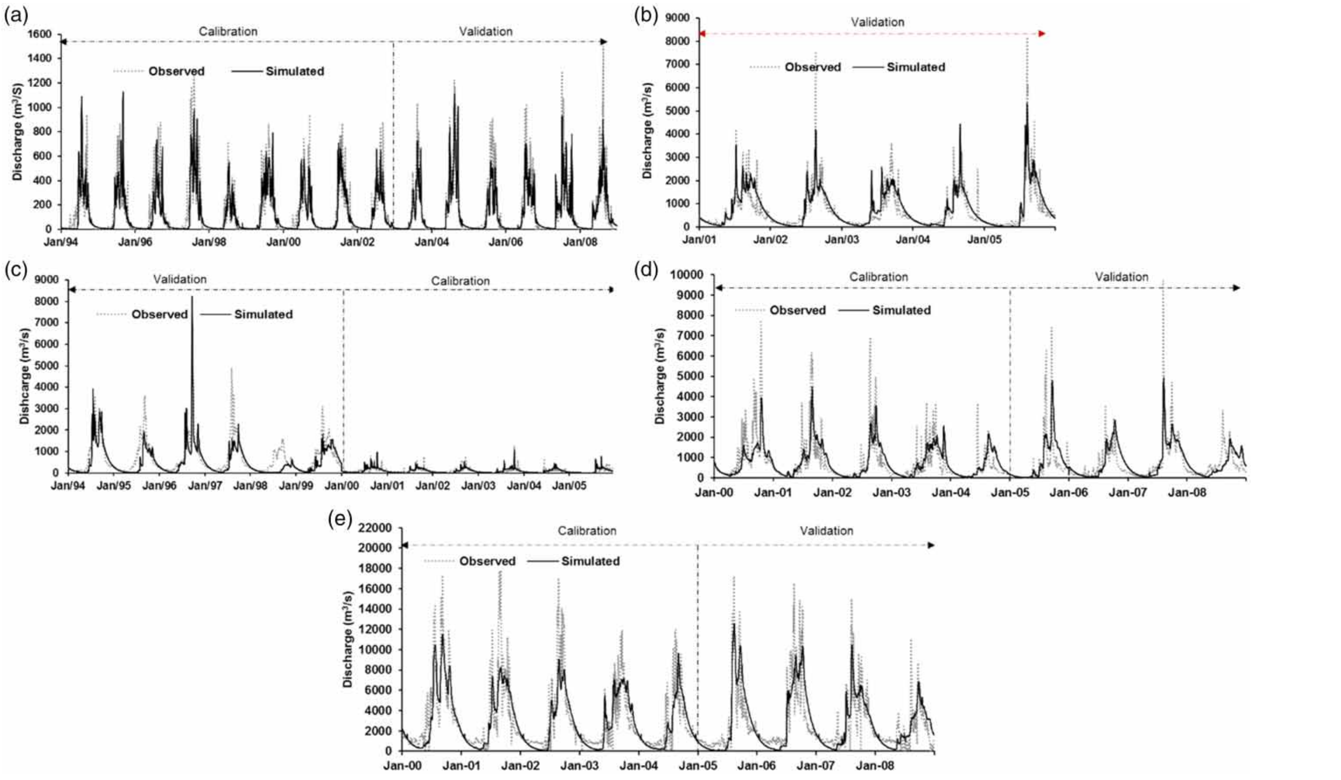

Figure 5 | Observed and simulated daily river discharge during calibration and validation of the SWAT model in tropical basins: (a) Bago, (b) Sekong, (c) Sesan, (d) Srepok and (e) 3S Basin.

River whereas it shows the highest overestimation for the Bago River during the calibration period. During the calibration period, the *NSE* and R^2 of the models ranges from 0.36 to 0.72 and 0.54 to 0.72, respectively. These values show that the model falls within the acceptable rating and that the SWAT model is therefore capable of capturing both the daily variation and pattern of discharge. Similarly, *PBIAS* and *RSR* also fall within the rating of 'good' with values ranging from −9.56 to 8.21% and 0.21 to 0.68, respectively.

The Sekong, Sesan and Srepok Rivers form the 3S River and were modelled as one basin and calibrated at the outlet first. The model was then recalibrated at each station of the three rivers, Sekong, Sesan and Srepok. Finally, the optimum set of model parameters was selected for the overall 3S River Basin. In this process, it can be seen that the statistical value of the 3S River outlet was much better than for the three individual rivers. Due to the limitation of data at the Sekong River, all the data were used for the validation period only.

During the validation period, the models performed better compared to the calibration period. All the statistical values lie within the rating of 'very good' and 'good'.

Hydrological extremes

As for the Himalayan basins, the *Q95* and *Q5* values were extracted for analysis of the tropical basin models. The Sekong and Srepok Basins show the best results in terms of low discharge simulation based on statistics R^2 and wR^2 (see Table 8). SWAT models for the Sesan and Belu Basins indicate either over- or underestimation of discharge, although the pattern of low discharge is followed well. For the 3S Basin (the combination of Sesan, Sekong and Srepok), there is a larger deviation in the low discharge simulations which is also visible from the hydrograph as well as the corresponding FDC and box plots in Figure 6. Due to the fact that most of the *Q95* values for the Bago Basin were zero, it was not possible to calculate the evaluation statistics.

On the other hand, the *Q5* discharge values show that the models for the Bago, Belu and Sekong Basins perform well in simulating the peak events. The location of upper whiskers is also seen to match better with that of the observed box plots. In the remaining three basins, the values show deviations as indicated by the rising end of their corresponding FDC and the upper whiskers of the box plots, even though they manage to get the pattern correct for the peaks (high values of R^2). Although most of the models for the tropical basins lag in either the flood events or low discharge, the SWAT model for the Sekong shows that a balanced hydrological model is possible.

Table 8 | Goodness-of-fit statistics of daily hydrological extremes simulated by the SWAT model in the tropical river basins

	Low discharge (*Q95*) statistics		High discharge (*Q5*) statistics		
Basin	R^2	wR^2	*NSE*	R^2	*RSR*
Bago, Myanmar[a]	–	–	0.666	0.981	0.578
Belu, Myanmar	0.955	0.002	0.836	0.953	0.405
Sekong, Laos	0.959	0.457	0.711	0.935	0.537
Sesan, Vietnam	0.862	0.162	0.141	0.841	0.927
Srepok, Cambodia	0.936	0.435	0.155	0.982	0.919
3S (Laos, Cambodia and Vietnam)	0.453	0.243	−2.464	0.992	1.861

[a]The observed low discharge data (*Q95*) mostly comprises zero discharge values; consequently, the statistics could not be calculated.

Sensitivity parameters

The sensitivity analysis results are summarised in Tables 9 and 10. Since all river basins in the Himalayan region originate from melting snow, it is obvious that the

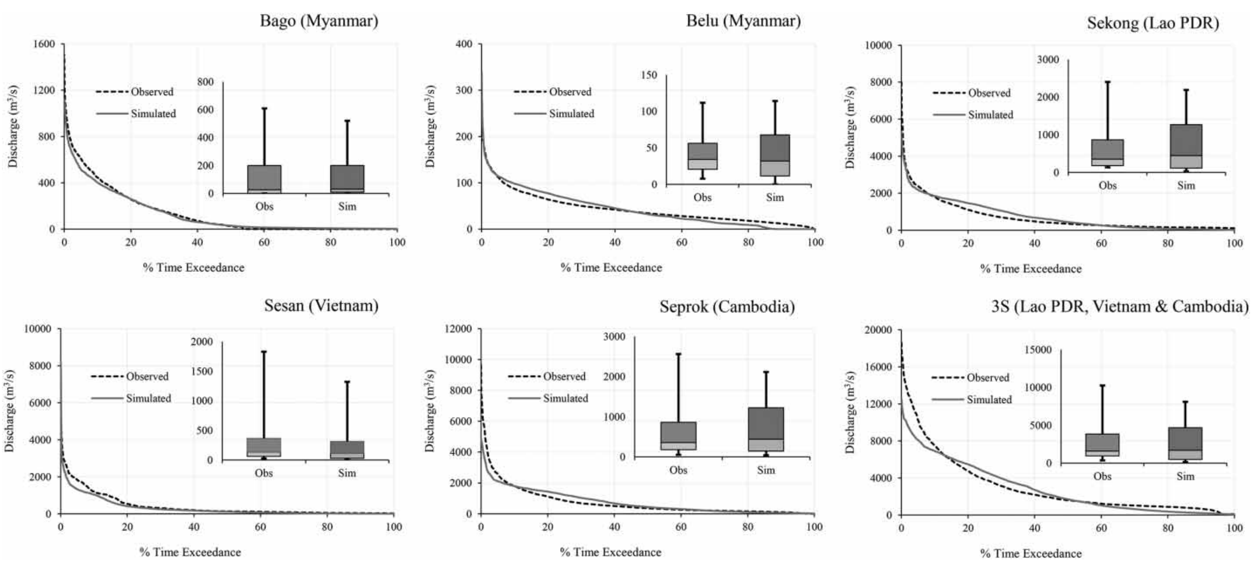

Figure 6 | Observed and simulated daily FDCs and quantile box plots of river discharge in the tropical basins.

Table 9 | The eight most sensitive SWAT parameters in the Himalayan basins. Numbers in parentheses show the fitted values of parameters in the corresponding basin

Rank	Indrawati	Melamchi	Tamakoshi	Tamor
1	TLAPS (−7)	TLAPS (−7)	TLAPS (−5.5)	Alpha_BF (0.185)
2	SFTMP (−0.5)	SFTMP (−0.5)	CH_K1 (79)	CH_N2 (0.019)
3	SMTMP (1.5)	SMTMP (1.5)	SFTMP (0.2)	CH_K2 (349.15)
4	Lat_Time (30)	Lat_Time (30)	CN2 (60–85)	GWQMN (774.2)
5	CANMX (3)	CANMX (3)	PLAPS (±150)	SNO50COV (0.536)
6	Alpha_BF (0.0128)	Alpha_BF (0.0128)	SOL_K (190)	TIMP (0.672)
7	GW_Delay (500)	GW_Delay (500)	SMFMX (9)	ECPO (0.767)
8	SNO50COV (0.5)	SNO50COV (0.5)	CH_K2 (267)	SOL_K (36–260)

Note: TLAPS: temperature lapse rate (°C/km); SFTMP: snowfall temperature; SMTMP: snowmelt base temperature; SMFM: maximum melt rate for snow during year (occurs on summer solstice); PLAPS: precipitation lapse rate (mm/km); Lat_Time: lateral flow travel time; CANMX: maximum canopy storage; Alpha_BF: baseflow alpha factor (days); GW_Delay: groundwater delay (days); SNO50COV: snow water equivalent that corresponds to 50% snow cover; CH_K1: effective hydraulic conductivity in tributary channel alluvium; CN2: initial runoff SCS curve number; SOL_K: saturated hydraulic conductivity (mm/hr); CH_K2: effective hydraulic conductivity in main channel (mm/h); CH_N2: Manning's n value for the main channel; GWQMN: threshold depth in the shallow aquifer required for return flow to occur; TIMP: snowpack temperature lag factor; ECPO: plant uptake compensation factor.

Table 10 | The eight most sensitive SWAT parameters in the tropical basins. Numbers in parentheses show the fitted values of parameters in the corresponding basin

Rank	Sekong	Sesan	Seprok	3S River	Bago	Belu
1	CN2 (55–84)	CN2 (55–84)	CN2 (55–84)	CN2 (55–84)	ESCO.hru (0.2)	CN2 (51–80)
2	SOL_K (1.4–8.07)	SOL_K (1.4–8.07)	SOL_K (1.4–8.07)	SOL_K (1.4–8.07)	CN_N1 (0.014)	CH_K2 (1.68)
3	SOL_Z (300)	SOL_Z (300)	SOL_Z (300)	SOL_Z (300)	ESCO.bsn (0.5)	GW_Delay (300)
4	CANMX (8.93)	CANMX (8.93)	CANMX (8.93)	CANMX (8.93)	REAVPMN (500)	ESCO.hru (0.85)
5	Alpha_BF (0.86)	Alpha_BF (0.86)	Alpha_BF (0.86)	Alpha_BF (0.86)	Alpha_BF (0.55)	Alpha_BF (0.048)
6	GW_Delay (49.61)	GW_Delay (49.61)	GW_Delay (49.61)	GW_Delay (49.61)	RCHRG_DP (0.6)	CH_N2 (0.014)
7	CH_K2 (146.61)	CH_K2 (146.61)	CH_K2 (146.61)	CH_K2 (146.61)	GW_Delay (10)	SOL_K (0.33–7.91)
8	CH_N2 (5.99)	CH_N2 (5.99)	CH_N2 (5.99)	CH_N2 (5.99)	GWQMN (0)	SOL_Z (400)

Note: CN2: initial runoff SCS curve number; SOL_K: saturated hydraulic conductivity (mm/hr); SOL_Z: soil depth (mm); CANMX: maximum canopy storage; Alpha_BF: baseflow alpha factor (days); GW_Delay: groundwater delay (days); CH_K2: effective hydraulic conductivity in main channel alluvium; CH_N2: Manning's n value for the main channel; ESCO.hru: soil evaporation compensation factor; CN_N1: Manning's n value for the tributary channels; ESCO.bsn: soil evaporation compensation factor; REAVPMN: threshold depth of water in the shallow aquifer for 'revap' or percolation to the deep aquifer to occur (mmH2O); RCHRG_DP: deep aquifer percolation fraction; GWQIMN: threshold depth of water in the shallow aquifer required for return flow to occur (mm H_2O).

parameters relating to snowfall and snowmelt play a vital role in calibration. The snowfall temperature (SFTMP parameter) determines the rainfall to be converted to snowfall. The snowfall is stored at the surface in the form of a snowpack and starts to melt once the snowpack temperature exceeds that of the snowmelt (SMTMP parameter) defined by the user. The snowpack temperature is the function of the previous day's temperature and current day snowpack temperature, controlled by a lagging factor (TIMP parameter). Similarly, the orographic effect on temperature and precipitation also plays a significant role in the Himalayan basins. Elevation bands were created for each of the sub-basins in the Himalayan region which helped to improve the discharge of the model. The temperature lapse rate (TLAPS parameter) and precipitation lapse rate (PLAPS parameter) determine the precipitation and temperature for each of the elevation bands. However, these parameters showed no effect in the tropical basins.

Soil parameters such as SOL_K (saturated hydraulic conductivity), SOL_AWC (available water capacity of the soil) and SOL_Z (soil depth), along with CN2 (initial runoff SCS curve number), Manning's n value and effective hydraulic conductivity for both main and tributary channels played a significant role in basins in the tropical region compared to the Himalayan. This might be due to the slow surface runoff compared to the Himalayan region, where water flows much faster compared to percolation. This can be further supported by the sensitivity of groundwater parameters like Alpha_BF (baseflow alpha factor), GW_Delay (groundwater delay), REVAPMN (threshold depth of water in the shallow aquifer to deep aquifer) and GWQIMN (threshold depth of water in the shallow aquifer required for return flow to occur).

CONCLUSIONS

This study evaluated the hydrological responses of SWAT models for 11 basins in two contrasting climatic regions of Asia. The results suggest that SWAT is a suitable tool for modelling hydrological responses over a wide range of basin scales, geographical regions and climatological settings.

For the Himalayan basins, a very good hydrographic fit was observed during the model calibration (*NSE*cal 0.72–0.81). Model period selection was attributed to underperformance in two of the basins during validation. Two major snow-fed basins showed high performance throughout the modelling years, supporting the argument that the SWAT model is capable of reproducing hydrological variations brought about by snowmelt. For hydrological extremes, two of the basins performed well in low discharge events, two performed well in simulating the peaks while one showed a balance between the extremes. In the case studies on tropical basins, SWAT showed good performance in fitting hydrographically (*NSE*cal 0.36–0.72). As in the Himalayan basins, five out of six models underperformed either in flood or low discharge events, but the one remaining showed a balance between the extremes. In summary, SWAT was found to be suitable for both climatic regions but performed better in the Himalayan basins.

Use of unconventional evaluation statistics (wR^2 and NSE_{rel}) in conjunction with the more established ones yielded better control of hydrological response/hydrograph evaluation. For extreme discharges, R^2 and wR^2 were successfully used to assess the low discharges while *NSE*, R^2 and *RSR* were enforced for high discharges. A trade-off effect was evident between the SWAT model performance for low and peak discharge in most of the basins. However, a couple of basins also demonstrated that a balanced hydrograph with SWAT is also possible via rigorous fine-tuning.

This multi-basin study with resulting parameterisation of the different basins yielded a useful table of model parameters for SWAT in the two contrasting geographical/climatological regions. It was found that parameters relevant to topographical variation and snow had higher sensitivity during model calibration for the Himalayan regions whereas parameters related to soil and groundwater were more sensitive for modelling in the tropical regions. However, it was also noted that although there is referable information regarding the sensitive parameters for a particular region, the complete set of sensitive parameters for each basin model were case specific. This kind of comprehensive multi-basin study highlighting model performance and parameterisation would help future researchers in developing the SWAT model in regions similar to those incorporated herein.

ACKNOWLEDGEMENTS

The authors would like to thank Ajay Bajracharya, Umubyeyi Safari Prosper, Minn Thu Aung, and Nguyen Thi Thuy Trang for allowing some of the outputs of their research to be incorporated in this paper, carried out under the Water Engineering and Management Program of the Asian Institute of Technology, Thailand.

REFERENCES

Abbaspour, K. C., Yang, J., Maximov, I., Siber, R., Bogner, K., Mieleitner, J., Zobrist, J. & Srinivasan, R. 2007 Modelling hydrology and water quality in the pre-alpine/alpine Thur watershed using SWAT. *Journal of Hydrology* **333** (2–4), 413–430. DOI: 10.1016/j.jhydrol.2006.09.014.

Arnold, J. G., Srinivasan, R., Muttiah, R. S. & Williams, J. R. 1998 Large area hydrologic modeling and assessment part I: model development. *Journal of the American Water Resource Association* **34** (1), 73–89.

Arnold, J. G., Moriasi, D. N., Gassman, P. W., Abbaspour, K. C., White, M. J., Srinivasan, R., Santhi, C., Harmel, R. D., van Griensven, A., Van Liew, M. W., Kannan, N. & Jha, M. K. 2012 SWAT: model use, calibration and validation. *Transactions of the ASABE* **55** (4), 1491–1508.

Aung, M. T., Shrestha, S., Weesakul, S. & Shrestha, P. K. 2015 Multi-model climate change projections for Belu River Basin, Myanmar under representative concentration pathways. *Journal of Earth Science & Climatic Change* **7** (1). DOI: 10.4172/2157-7617.1000323.

Beskow, S., Mello, C. R., Norton, L. D. & da Silva, A. M. 2011 Performance of a distributed semi-conceptual hydrological model under tropical watershed conditions. *Catena* **86**, 160–171. DOI: 10.1016/j.catena.2011.03.010.

Cornelissen, T., Diekkrüger, B. & Giertz, S. 2013 A comparison of hydrological models for assessing the impact of land use and climate change on discharge in a tropical catchment. *Journal of Hydrology* **498**, 221–236. DOI: 10.1016/j.jhydrol.2013.06.016.

Dobler, C., Bürger, G. & Stötter, J. 2012 Assessment of climate change impacts on flood hazard potential in the Alpine Lech watershed. *Journal of Hydrology* **460–461**, 29–39. DOI: 10.1016/j.jhydrol.2012.06.027.

Easton, Z. M., Fuka, D. R., White, E. D., Collick, A. S., Biruk Ashagre, B., McCartney, M., Awulachew, S. B., Ahmed, A. A. & Steenhuis, T. S. 2010 A multi basin SWAT model analysis of runoff and sedimentation in the Blue Nile, Ethiopia. *Hydrology and Earth System Sciences* **14**, 1827–1841. DOI: 10.5194/hess-14-1827-2010.

Francesconi, W., Srinivasan, R., Pérez-Miñana, E., Willcock, S. P. & Quintero, M. 2016 Using the Soil and Water Assessment Tool (SWAT) to model ecosystem services: a systematic review. *Journal of Hydrology* **535**, 625–636. DOI: 10.1016/j.jhydrol.2016.01.034.

Grusson, Y., Sun, X., Gascoin, S., Sauvage, S., Raghavan, S., Anctil, F. & Sáchez-Pérez, J.-M. 2015 Assessing the capability of the SWAT model to simulate snow, snow melt and streamflow dynamics over an alpine watershed. *Journal of Hydrology* **531**, 574–588. DOI: 10.1016/j.jhydrol.2015.10.070.

Krause, P., Boyle, P. & Base, F. 2005 Comparison of different efficiency criteria for hydrological model assessment. *Advances in Geosciences* **5**, 89–97.

Krysanova, V. & White, M. 2015 Advances in water resources assessment with SWAT – an overview. *Hydrological Sciences Journal* **60**, 771–783.

Majone, B., Bertagnoli, A. & Bellin, A. 2010 A non-linear runoff generation model in small Alpine catchments. *Journal of Hydrology* **385**, 300–312. DOI: 10.1016/j.jhydrol.2010.02.033.

Moriasi, D. N., Arnold, J. G., Van Liew, M. W., Bingner, R. L., Harmel, R. D. & Veith, T. L. 2007 Model evaluation guidelines for systematic quantification of accuracy in watershed simulations. *American Society of Agricultural and Biological Engineers* **50**, 885–900.

Ndomba, P., Mtalo, F. & Killingtveit, A. 2008 SWAT model application in a data scarce tropical complex catchment in Tanzania. *Physics and Chemistry of the Earth, Parts A/B/C* **33**, 626–632. DOI: 10.1016/j.pce.2008.06.013.

Neitsch, S. L., Arnold, J. G., Kiniry, J. R., Williams, J. R. & King, K. W. 2011 *Soil and Water Assessment Tool (Version 2000)–Theoretical Documentation*. Grassland, Soil and Water Research Laboratory, Agricultural Research Service, Blackland Research Center, Texas Agricultural Experiment Station, Temple, TX.

Neupane, R. P., Yao, J. & White, J. D. 2014 Estimating the effects of climate change on the intensification of monsoonal-driven stream discharge in a Himalayan watershed. *Hydrological Processes* **28**, 6236–6250.

Neupane, R. P., White, J. D. & Alexander, S. E. 2015 Projected hydrologic changes in monsoon-dominated Himalaya Mountain basins with changing climate and deforestation. *Journal of Hydrology* **525**, 216–230. DOI: 10.1016/j.jhydrol.2015.03.048.

Pereira, D. d. R., Martinez, M. A., da Silva, D. D. & Pruski, F. F. 2016 Hydrological simulation in a basin of typical tropical climate and soil using the SWAT model part II: simulation of hydrological variables and soil use scenarios. *Journal of Hydrology: Regional Studies* **5**, 149–163. DOI: 10.1016/j.ejrh.2015.11.008.

Plesca, I., Timbe, E., Exbrayat, J. F., Windhorst, D., Kraft, P., Crespo, P., Vaché, K. B., Frede, H. G. & Breuer, L. 2012 Model intercomparison to explore catchment functioning: results from a remote montane tropical rainforest. *Ecological Modelling* **239**, 3–13. DOI: 10.1016/j.ecolmodel.2011.05.005.

Rocha, F. A. 2016 Peer review report 1 On 'hydrological simulation in a basin of typical tropical climate and soil using the SWAT model part II: simulation of hydrological variables and soil use scenarios'. *Journal of Hydrology: Regional Studies* **5**, 51. DOI: 10.1016/j.ejrh.2016.01.015.

Rodrigues, L. 2016 Peer review report 2 On 'hydrological simulation in a basin of typical tropical climate and soil using the SWAT model part II: simulation of hydrological variables and soil use scenarios'. *Journal of Hydrology: Regional Studies* **5**, 52. DOI: 10.1016/j.ejrh.2016.01.016.

Shrestha, N. K., Leta, O. T., De Fraine, B., van Griensven, A. & Bauwens, W. 2013 Open MI-based integrated sediment transport modelling of the river Zenne, Belgium. *Environmental Modelling & Software* **47**, 193–206. DOI: 10.1016/j.envsoft.2013.05.004.

Shrestha, S., Shrestha, M. & Babel, M. S. 2016 Modelling the potential impacts of climate change on hydrology and water resources in the Indrawati River Basin, Nepal. *Environmental Earth Sciences* **75**, 280. DOI: 10.1007/s12665-015-5150-8

Shrestha, S., Shrestha, M. & Babel, M. S. 2017 Assessment of climate change impact on water diversion strategies of Melamchi Water Supply Project in Nepal. *Theo. Applied Clim*. **128** (1–2), 311–323. DOI: 10.1007/s00704-015-1713-6.

Singh, R. K., Panda, R. K., Satapathy, K. K. & Ngachan, S. V. 2011 Simulation of runoff and sediment yield from a hilly watershed in the eastern Himalaya, India using the WEPP model. *Journal of Hydrology* **405**, 261–276. DOI: 10.1016/j.jhydrol.2011.05.022.

Yira, Y., Diekkrüger, B., Steup, G. & Bossa, A. Y. 2016 Modeling land use change impacts on water resources in a tropical West African catchment (Dano, Burkina Faso). *Journal of Hydrology* **537**, 187–199. DOI: 10.1016/j.jhydrol.2016.0.

First received 29 June 2016; accepted in revised form 9 March 2017. Available online 21 April 2017